Dual Polarized Near Field Probe Based on OMJ in Waveguide Technology Achieving More Than Octave Bandwidth

L.J. Foged, A. Giacomini, R. Morbidini, V. Schirosi
MICROWAVE VISION ITALY
Via Castelli Romani, 59
00040 Pomezia (Rome), ITALY
lars.foged@microwavevision.com

S. Pivnenko
TECHNICAL UNIVERSITY OF DENMARK
Department of Electrical Engineering
Ørsteds Plads, Building 348,
2800 Kgs. Lyngby, DENMARK
sp@elektro.dtu.dk

***Abstract* — In classic probe-corrected spherical NF measurements, one of the main concerns is the probe [1], [2], [3]. Standard NF-FF transformation software applies probe correction with the assumption that the probe pattern behaves with μ=±1 azimuthal dependence. In reality, any physically realizable probe is just an approximation to this ideal case. Probe excitation errors, finite manufacturing tolerances and probe interaction with the mounting interface and absorbers are examples of uncertainties that can lead to presence of higher-order spherical modes in the probe pattern [4], [5]. Although probe correction techniques for high-order probes are feasible [6], they are highly demanding in terms of implementation complexity as well as in terms of calibration and post-processing time. In this paper, a new OMJ designed entirely in waveguide and capable of covering more than an octave bandwidth is presented. The excitation purity of the balanced feeding is limited only by the manufacturing accuracy of the waveguide. The paper presents the waveguide based OMJ concept including probe design covering the bandwidth from 18 to 40 GHz using single and dual apertures. The experimental validation is completed with measurements on the dual aperture probe at the DTU-ESA Spherical Near-Field facility in Denmark.**

I. INTRODUCTION

Dual polarized probes for modern high accuracy measurement systems have strict requirements in terms of pattern shape, polarization purity, return loss and port-to-port isolation. As a desired feature of modern probes the useable bandwidth should exceed that of the antenna under test so that probe mounting and alignment is performed only once during a measurement campaign [1]. As a consequence, the probe design is a trade-off between performance requirements and usable bandwidth. High performance, dual polarized probes rely on balanced feeding in the OMJ to achieve good performance on a wide, more than an octave, bandwidth [5], [7], [8]. Excitation errors of the balanced feeding must be minimized to reduce the excitation of higher order spherical modes. Balanced feeding on a wide bandwidth has been mainly realized with external feeding network.

II. PROBE TECHNOLOGY

The probe technology described in this section is based on a balanced feeding technique, four feeding points with proper phasing exciting a wideband ortho-mode junction (OMJ) as shown in Fig.1. A key point is the targeted 18-40 GHz operational bandwidth thus, more than an octave bandwidth. Conventional hollow waveguides usually considered at Ka-band are to be replaced with wider bandwidth single/dual ridge waveguides.

A cascade of microwave building blocks composes each probe channel: connectorized launcher, E-plane splitter, side arms (two for each polarization), balanced OMJ and radiating apertures. The apertures can either be intended to cover the full 18-40GHz band in a single aperture or can be designed for different radiation characteristics on different sub-bands like the dual aperture probe presented in this paper covering 18-26GHz and 26-40GHz, respectively. The interface between OMJ and radiating aperture is specifically designed to support apertures of different dimensions depending on the application scenario. The aperture substitution has no impact on the probe alignment, since the precision mounting interface is "one piece" with the OMJ. Each probe component will be discussed in detail in the following.

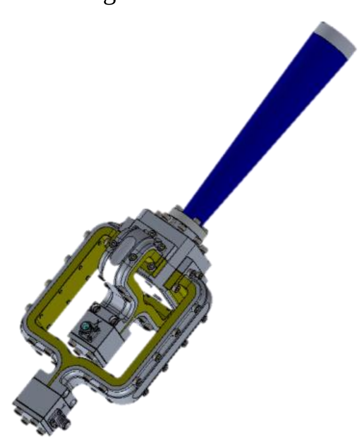

Figure 1. Main structure of the dual polarized probe.

The launcher is a connectorized transition from K-type coaxial interface to a dual ridge waveguide with custom designed cross-section. The excitation is based on a capacitive pin, proximity coupled to the dual ridge waveguide section as shown in Fig 2 (left). Such transitions are inherently asymmetric and therefore unbalanced, but careful tuning of the design ensures pure mono-mode excitation and matching over the operational bandwidth. The dual ridge waveguide is then mated to an E-plane splitter which bifurcates the dual ridge waveguide into two single ridge waveguides with identical cross-section as shown in Fig 2 (right).

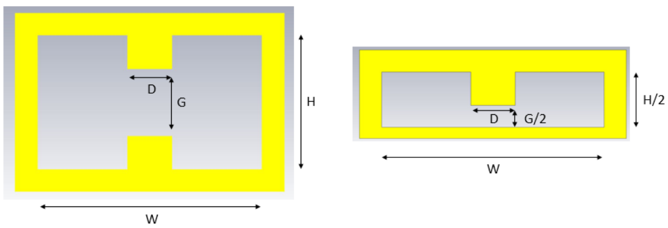

Figure 2. Section of a dual ridge waveguide (left). Section of a single ridge waveguide (right).

Ideally, a split dual ridge waveguide can be obtained by means of an infinitely thin metal blade located in the waveguide H-plane with equal distance from upper and lower walls. Amplitude and phase imbalance, as well as matching, is ideal in this case. Considering manufacturing constraints, the metal blade will have a finite thickness, which is to be compensated by tuning the blade position and dimensions of the single ridge waveguide cross-sections: R, G and t, as shown in Fig. 3. This is done to achieve a good impedance matching and to avoid the excitation of higher order modes. The resulting design is depicted in Figure 4.

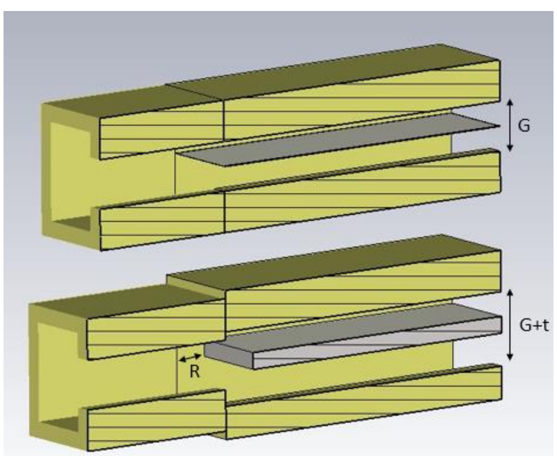

Figure 3. Section view of the splitting principle of a dual ridge waveguide in two single ridge waveguides. Ideal case (on the top), real case (on the bottom).

The split signals are then conducted through the two side arms and bends to the OMJ. The proposed OMJ design is an evolution of a classic turnstile junction [9], using ridge waveguides as four points feeding section and an oversized coaxial structure as common waveguide as shown in Fig. 5.

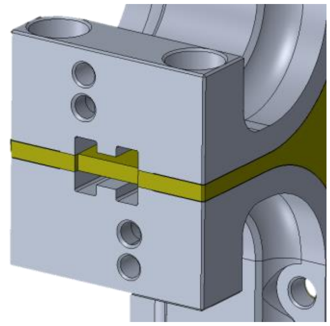

Figure 4. E-plane splitter without the connectorized launcher.

The shape of the coaxial waveguide allows to control the impedance matching and the modal conversion by means of a tapering of the inner conductor and of the external walls of the aperture (Figure 5). Apertures can have different shapes (conical or corrugated) and dimensions, depending of the operational bandwith and on the pattern characteristic to be synthesized.

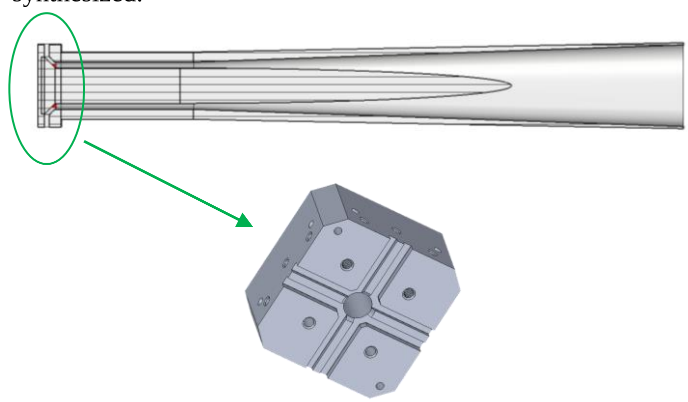

Figure 5. Transition between the single ridge waveguides (four feeding points) and the oversized coaxial waveguide.

III. ENGINEERING MODEL

The engineering model shown in Fig. 6 is composed of an assembly of building blocks, each manufactured from solid Al alloy with high precision CNC machining (milling/turning), inter-connected by means of waveguide flanges.

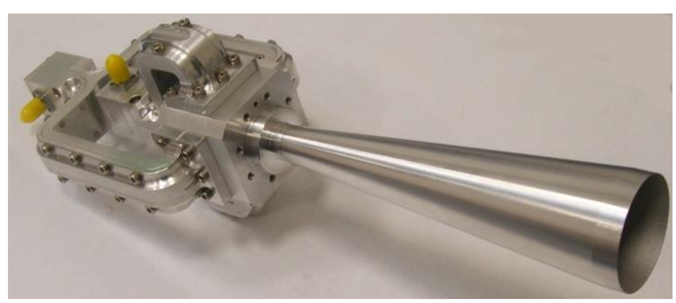

Figure 6. Engineering Model

The most critical segment for manufacturing aspects is represented by the single ridge side arms feeding the OMJ. The selected approach for these sections is based on the use of clamshells, as depicted in Fig. 7.

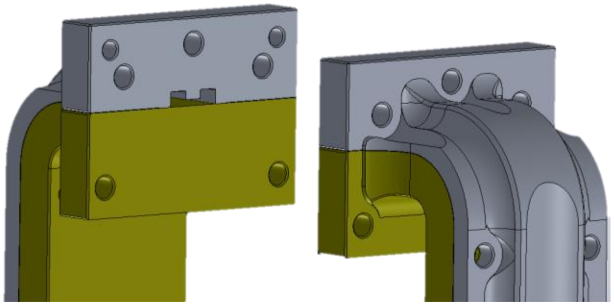

Figure 7. Single ridge side arms manufactured as clamshells (OMJ flanges).

In traditional clamshell waveguide manufacturing, the common practice is to split the rectangular hollow waveguide along the E-plane. The reason is that the mechanical junctions between the clamshells should never be orthogonal to the currents flowing on the inner surfaces of the waveguide. While this approach is straight forward for rectangular waveguides, dividing them into two “U” shaped halves for assembly, this is more critical for single/dual ridge waveguides. The ridge parts of the waveguide become very thin by this division and difficult to join together and the two halves present a more difficult geometry to machine. For the engineering model, it was decided for simplicity to divide the side arms as shown in Fig. 7.

The ohmic contact between the two clamshells is foreseen to be critical, a contact lip and several tightening screws have been added all over the perimeter to ensure good contact. In fact, a poor contact between the shells will result in leakage from the guiding structures and unwanted excitation of higher order modes, determining uncontrolled amplitude/phase response of the side arms.

IV. MEASUREMENTS

Prior to assembly of the probe and successive antenna pattern verification, the individual parts of the BFN assembly have been assembled and tested separately. An important test was conducted on the feeding sections of the probe composed by the launcher, the E-plane splitter and the side arms. The purpose was to verify that the expected balanced feeding law had been achieved in the design bandwidth. Amplitude and phase balance over frequency for both polarizations has been measured, removing the effect of the test set-up for accurate results. The Y-polarization results are shown in Fig. 8, similar results have been obtained for the X-polarization.

The amplitude difference pattern between the two branches shows an average value close to zero as expected, this is a clear indication that the geometrical symmetry of the E-plane splitter is satisfactory. Some high frequency ripple with ±0.3 dB amplitude is visible and is an indication of minor discontinuities along the side arms. Observing the phase difference pattern, the distribution shows a 1/f trend, and is probably due to a leakage phenomenon at low frequency from the side arms.

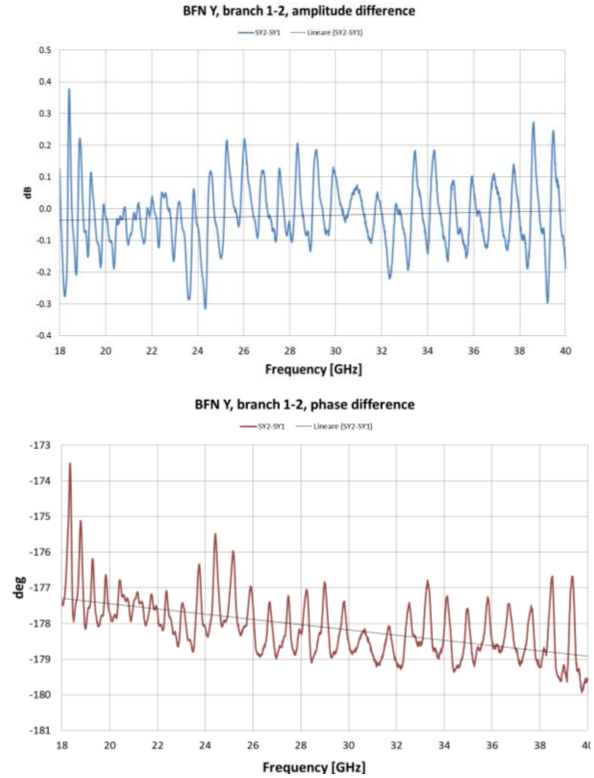

Figure 8: Measured amplitude and phase difference between both feeding network branches for Y-polarization.

Although the measured amplitude and phase balance of the feeding network is considered excellent, the occurrence of leakage was further investigated to verify the quality of the ohmic contact in the feeding network. The level of leakage was measured by a rectangular open ended waveguide along the side arms, according to the points indicated in Fig. 9.

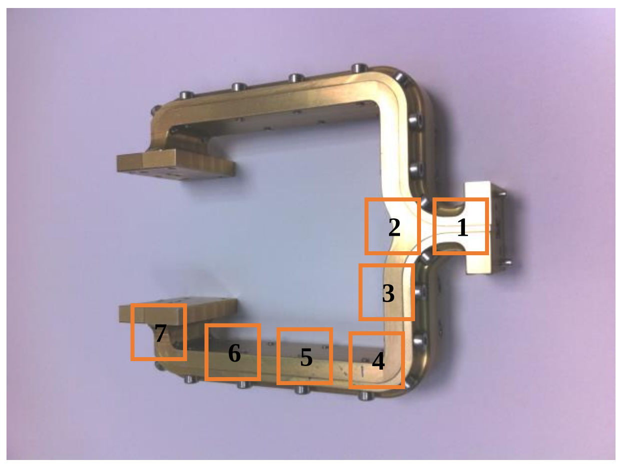

Figure 9: Areas along the BFN where the leakage measurements have been conducted.

The measured leakage in point #5 is shown in Fig. 10. As expected, the measurements show that some leakage occurs at lower frequencies due to the non-ideal contact between the clam shells. The leakage is more evident at lower frequencies.

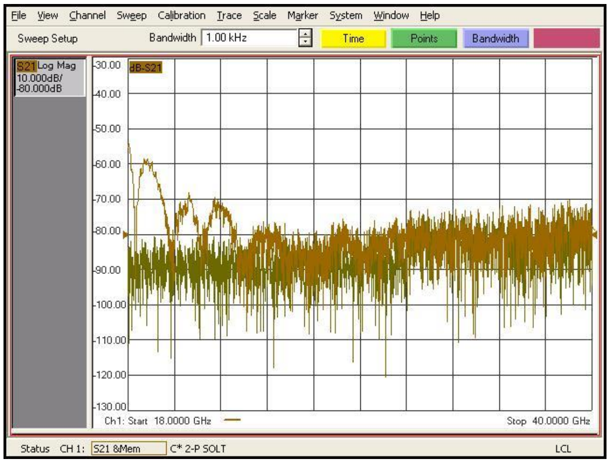

Figure 10. Leakage measurements corresponding to point 5 of the Y polarization branch (green trace is the noise floor).

The final assembled probe is shown in Fig. 6. The probe including absorber panel and mounted on the AUT positioner is shown in Fig. 11 during testing at the DTU-ESA Spherical Near-Field facility in Denmark. The complete testing included S-parameters, Gain, Directivity and Patterns.

The testing at the DTU-ESA Facility was performed with exchangeable probe apertures, each specifically optimized for radiation pattern properties on the 18-26GHz (aperture#1) and 26-40GHz (aperture#2) sub-bands. The division in sub-bands and hence two apertures, is motivated with a desired specific narrow range of probe gain between 16-19dBi. However, the entire frequency range 18-40GHz can be covered by each of the apertures if needed.

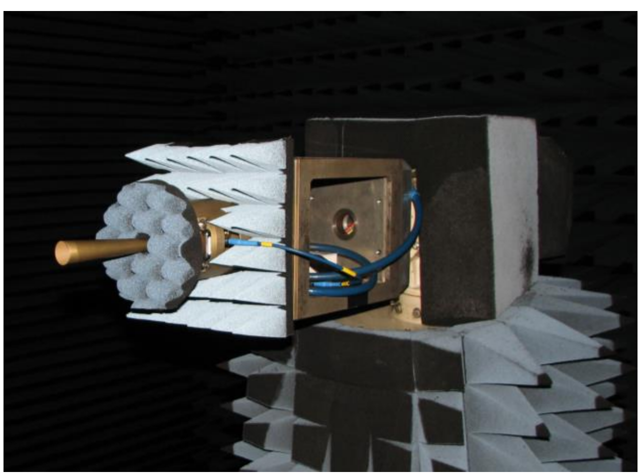

Figure 11: Test set-up in DTU Spherical Near-Field facility.

The measured return loss for each port and port-to-port coupling for the dual polarized probe with aperture #1 and aperture #2 are shown in Fig. 12. The measurements show that the target 10dB or better return loss has been achieved for both ports and with both apertures. The measured port-to-port isolation is also satisfactory with levels better than 50/60dB. The performance is slightly better with the aperture #1 designed for the 18-26GHz range probably due to the narrower dimensions of this aperture.

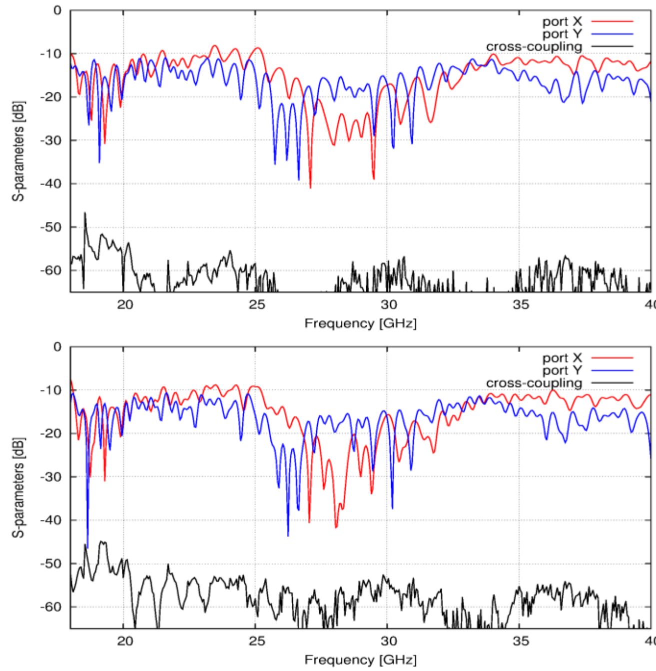

Figure 12. S-parameter performance of the probe measured at the DTU-ESA facility. Probe with Aperture #1 (top) and Probe with aperture #2 (below).

The measurement at the DTU-ESA Spherical Near-Field facility of the probe radiation characteristics was carried out for each polarization port separately, with the unused port terminated in a 50Ohm load. For each polarization port, a full-sphere data set was acquired. During NF-FF transformation and data post-processing a small translation of the AUT (wide-band probe) reference coordinate system along the x and y-axis was applied to correct for mounting tolerances of the test mechanical interface [4]. The correction has no impact on the probe far-field pattern, but unless corrected leads to variations in the probe modal content.

The measured peak directivity of the probe with different apertures is shown in Fig. 13 on the 18-40GHz operating bandwidth. The desired range of 16-19dBi has been achieved on each sub-band.

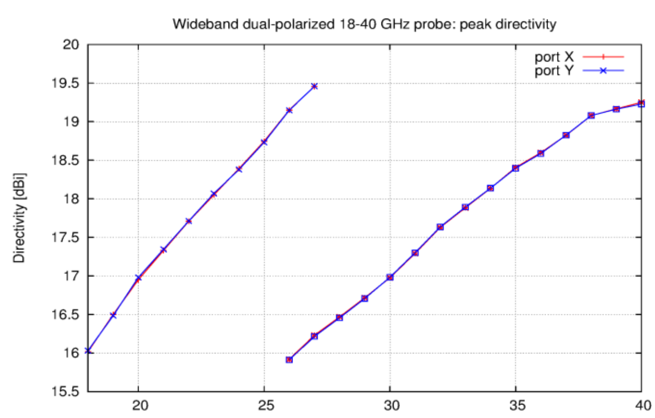

Figure 13. Measured directivity for aperture 1 (curve on the left) and for aperture 2 (on the right).

Examples of the measured radiation pattern in the principal planes at each of the extreme frequencies of the defined apertures are shown in Fig. 14 and Fig. 15 respectively. The pattern symmetry is very nice at all frequencies but the on-axis cross polar levels are higher than expected. This higher cross-polar levels are probably due to the measurement and is still being investigated.

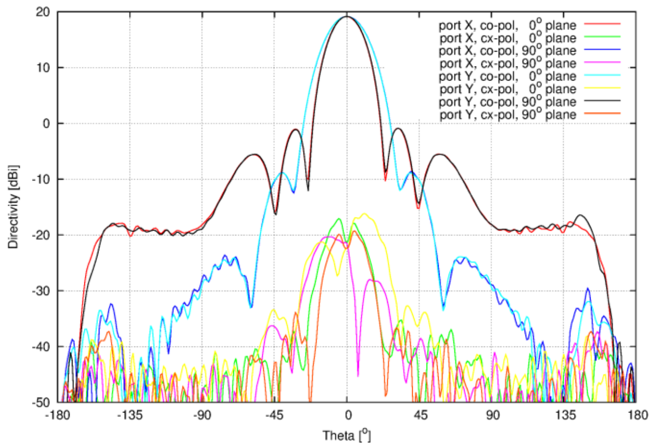

Figure14. Far-field pattern at 26 GHz (aperture 1).

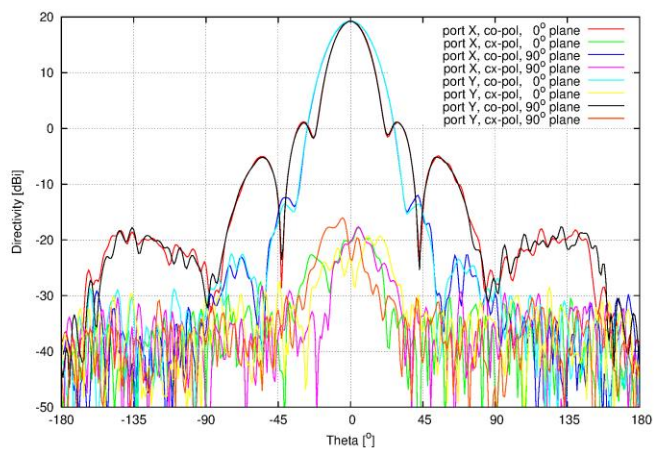

Figure 15. Far-field pattern at 40 GHz (aperture 2).

The spherical mode coefficients have been calculated from the measured radiation pattern in order to understand how close the proposed design is to a theoretical $\mu=\pm1$ probe. The modal content also gives some indication on how well the waveguide OMJ controls the excitation of the balanced feeding. A small translation of the reference coordinate system along the x and y-axes was applied to correct for mounting tolerances of the test mechanical interface [4].

The modal content for discrete frequencies from 33GHz to 40GHz for aperture #2 is shown in Fig 16. While the spectrum indices $\mu=0$ and $\mu=2$ are -35dB, the modal spectrum with indices $\mu>2$ is well below -40dB. Such values are generally associated with natural narrow band $\mu=\pm1$ probes. The modal spectrum of the measured probe thus confirms the expectations for such probe showing that the performance is very close to $\mu=\pm1$ on a wide bandwidth.

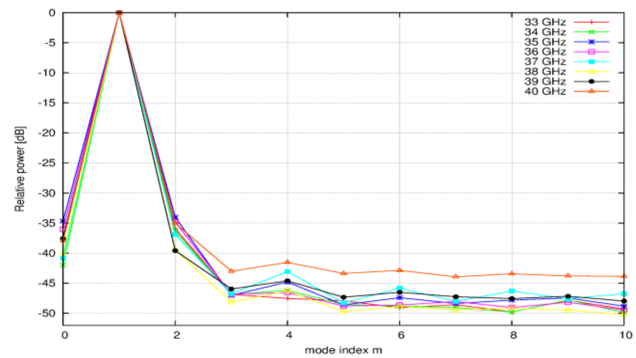

Figure 16. Measured modal content from 33 - 40 GHz (aperture 2).

V. Conclusions

A dual polarized, high frequency, wideband probe suitable for high accuracy near field antenna measurement application, was presented. The innovative feature of the design is represented by a novel OMJ, thought as an evolution of a classical turnstile junction. The presented design achieves very accurate balanced feeding without external components on the bandwidth from 18 to 40GHz. The predicted performances are confirmed by measurement. The reduced exitation errors and the associated reduction in higher order modal content are confirmed.

Other manufacturing processes are under investigation to avoid shells in the probe assembly. Such architecture will further reduce the leakage leading to an improvement in the balanced feeding and therefore the modal content.

Acknowledgements

The authors wish to thank Luc Duchesne from SATIMO Industries for helpful discussions and suggestions.

References

[1] IEEE Standard Test Procedures for Antennas, IEEE Std 149-1979.

[2] Reccomended Practice for NF Antenna Measurement, IEEE 1720-2012.

[3] J.E. Hansen (ed.), Sperical Near-Field Antenna Measurements, Peter Peregrinus Ltd., on behalf of IEE, London, UK, 1988.

[4] L.J. Foged, A. Giacomini, R. Morbidini, J. Estrada, S. Pivnenko, "Design and experimental verification of Ka-band Near Field probe based on wideband OMJ with minimum higher order spherical mode content", 34th Annual Symposium of the Antenna Measurement Technique Association, AMTA, Oct. 2012, Seattle, Washington, USA.

[5] L.J. Foged, A. Giacomini, R. Morbidini, "Probe performance limitation due to excitation errors in external beam forming network", 33rd Annual Symposium of the Antenna Measurement Techniques Association, AMTA, October 2011, Englewood, Colorado, USA.

[6] T. Laitinen, S. Pivnenko, J.M. Nielsen, and O. Breinbjerg, "Theory and practice of the FFT/matrix inversion technique for probe-corrected spherical near-field antenna measurments with high-order probes", IEEE Trans. Antennas Propag., vol. 58, no. 8, pp. 2623-2631, Aug. 2010.

[7] L.J. Foged, A. Giacomini, R. Morbidini, "Wideband dual polarized open-ended waveguide probe", AMTA 2010 Symposium, October, Atlanta, Georgia, USA.

[8] L.J. Foged, A. Giacomini, R. Morbidini "Wideband Field Probes for Advanced Measurment Applications", IEEE COMCAS 2011, 3rd International Conference on Microwaves Communications, Antennas and Electronic Systems, Tel-Aviv, Israel, November 7-9, 2011.

[9] Uher, J. Bornemann, U. Rosenberg "Waveguide Components for Antenna Feed Systems: Theory and CAD", Artech House, Chapter